## POLITECNICO DI TORINO
## Repository ISTITUZIONALE

A synthetic guide toward the tailored production of magnetic iron oxide nanoparticles

*Terms of use:*

*Publisher copyright*

(Article begins on next page)

25 April 2024
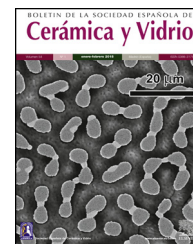
**Original**

# A synthetic guide toward the tailored production of magnetic iron oxide nanoparticles

*Roberto Nisticò*

*Independent Researcher, via Borgomasino 39, 10149 Torino, Italy*

## ARTICLE INFO

## ABSTRACT

In the last decades, magnetic ceramics are very appealing materials that find applications in several technologic fields. Among these, iron oxides nanoparticles are the main relevant ones due to their low-cost as naturally occurring substrates. However, depending on the application, it can be necessary to induce a specific shape and size control over the final morphology, and consequently a proper synthetic route becomes mandatory. Hence, this document provides a summary of the main relevant chemical, physical, thermal, and biological methods to induce a certain degree of morphological control in iron oxides. The main focus of this document relies on highlighting the principal guidelines, unveiling both advantages and disadvantages of each method in terms of morphology control in the resulting products. Lastly, a particular emphasis has been dedicated toward the industrial feasibility of all processes here discussed.

## Una guía sintética hacia la producción a medida de nanopartículas magnéticas de óxidos de hierro

### RESUMEN

En las últimas décadas, la cerámica magnética es un material muy atractivo que encuentra aplicaciones en varios campos tecnológicos. Entre estos, las nanopartículas de óxidos de hierro son las principales por su bajo costo como sustratos naturales. Pero, dependiendo de la aplicación, puede ser necesario inducir un control de forma y tamaño específico sobre la morfología final y, por lo tanto, una ruta sintética adecuada se vuelve obligatoria. Por esta razón, este documento ofrece un resumen de los principales métodos químicos, físicos, térmicos y biológicos relevantes para inducir un cierto grado de control morfológico en los óxidos de hierro. El objetivo principal de este documento se basa en resaltar las principales

## Introduction

Since from the early birth of human history, ceramic materials have proved to be a fundamental resource that favored the primitives' technological evolution and civilization [1,2]. Ceramics can be classified into either traditional (mostly made by a various combination of clays, silica, alumina and other oxides, used for the manufacturing of earthenwares, whitewares, stonewares, cements, concretes, mortars, and refractory materials) [3–6] or advanced (engineering, functional) ceramics (which are nearly pure compounds, such as oxides, carbides and nitrides, characterized by showing particular physical features) [7–10]. Furthermore, advanced ceramics can be divided into advanced structural ceramics (i.e., bioceramics, and tribological ceramics) and in electroceramics (i.e., electronic substrates, piezoelectric, optical, conductive, and magnetic ceramics) [11]. In this context, magnetic ceramics are a particular class of inorganic materials showing magnet-sensitive responses, very appealing for several technological applications since merging the advantages of their ceramic-nature (high-electrical resistivity, resistance to corrosion and wear) with being magnetics [12].

As reported in the literature, the EU market of permanent magnets is a continuously growing market segment, and its values has been estimated being more than $ 1100 million by 2018, thus making it a very promising technological field of research [13]. Such growing interest for advanced magnetic materials is also justified by the important technological milestones reached thanks to the implementation of magnet-based devices (e.g., the development of magnetic levitation-based MAGLEV trains for high-speed transport, or the magnetic therapy for the treatment of pain in biomedicine) [14,15]. According to the "*Modern Theory of Magnetism*" the production of a magnetic field in materials is determined by the electronic configuration (i.e., the distribution of the electrons in orbitals) and the electrons' spin motion [16,17]. These definitions pointed out two relevant facts: (i) magnetic phenomena arises directly from the electron motions, thus suggesting a strict correlation between magnetic field and electric field [18,19], and (ii) chemical elements with an electronic configuration able to guarantee a magnetic response in materials are only few transition metals, such as iron (Fe), nickel (Ni), cobalt (Co), manganese (Mn), and chromium (Cr), as well as some Rare Earths (RE) metals [20].

Basing on these axioms, considering the (electro)ceramics categories, the main relevant magnetic materials are ferrites and iron oxides (in different phases) [21,22]. Ferrites are a class of ceramic oxides, with general formula $MFe_2O_4$, where M is a general metal, different from Fe (i.e., if M is Fe(II) it generates a particular subclass of ferrites named magnetite, or $Fe_3O_4$) [17]. Furthermore, ferrites can be classified on their crystallographic structure as spinel- (the main relevant ones), garnet-, hexa- and ortho-ferrites, showing the presence of both octahedral and tetrahedral sites (i.e., two interpenetrating substructures) [23]. The position of the M/Fe heteroatoms within the crystal lattice influences the magnetic properties of spinel ferrites, and such structural organization depends on several parameters, such as: the nature of cations (ionic radius and valence), lattice's interstices (size), temperature, and electrostatic energy [24].

Even if ferrites occupy the majority of the magnetic ceramics' market, iron oxides still deserve a particular interest since being versatile, low-cost naturally occurring materials showing a quite high magnetic response [17]. In detail, iron oxides nanoparticles attracted worldwide researchers not only in magnetic devices (as ferrites do), but mainly due to their wide potential applications in waste/groundwater clean-up processes, sensing, drug-delivery and biomedicine, cosmetics, automotive, imaging, and so on. Additionally, iron oxide NPs are one of the main used nanoscopic contrast agents for magnetic resonance imaging (MRI) approved for clinical use [25]. However, depending on the crystal phase organization, it is possible to induce a different magnetic response (in the sense of different magnetism).

Therefore, aim of this study is to summarize the main relevant synthetic protocols found in the literature for obtaining specific magnetic phases with controlled geometries and dimensions. After providing a general overview on the concept (and principles) of magnetism, the iron oxide crystal phases were presented and the chemical/physical/thermal/biological methods critically discussed, highlighting their advantages and disadvantages in terms of control degree in the resulting products' morphology. Since this topic is transversal, this author tried to focus the discussion on the crystal structure-magnetism correlation, and on the chemical mechanisms driving the iron oxides' synthesis. For a more extensive (and generalist) discussion, this author suggests the following references as supporting literature [26,27].

## Magnetism and ceramics: a general overview

On the basis of the current literature, the main relevant forms of magnetism (characterized by having a macroscopic magnetic response) are basically two: ferromagnetism and ferrimagnetism. Ferromagnetism, which is the most intense form of magnetism, is a spontaneous magnetic phenomenon generated by the self-alignment of unpaired (same-spin) electrons forming the electronic configuration of the compound (typically, metallic forms of transition metal such as: Fe, Co, Ni, Cr, Mn, and some rare earths) [27]. At short level, ferromagnets are organized into magnetic domains generated by energetically favored coupling of nearby electrons. At high scale and in absence of an external magnetic field applied, these domains

are randomly-organized, following an anti-alignment organization (of adjacent poles). The main feature of ferromagnets is the capability of align domains parallel to the direction of the external magnetic field (once applied) and maintain a "memory" of this induced orientation, even after the removal of such external magnetic source [27,28]. Ferromagnetic materials are generally recognized being either hard- (or permanent) or soft-magnet (i.e., subjected to fast/easy magnetization-demagnetization) [29,30]. This capability is expressed by the coercivity ($H_c$) parameter, which is defined as the reverse magnetic field necessary to nullify the (volume) magnetization (M, i.e., the amount of magnetic moments per unit of volume). Furthermore, temperature affects ferromagnetism. In fact, for every ferromagnetic material, a critical temperature value (named Curie point, $T_c$) is defined: above this value, materials evolved toward a more disordered magnetic organization (i.e., paramagnetism) due to the thermally-induced uncontrolled motions of electrons, and consequently loss of magnetic-domains organization. This inter-magnetism transition is reversible [31].

Ferrimagnetism, instead, consists in a structure-related form of magnetism, which occurs in materials formed by two interpenetrating chemical structures showing an anti-alignment of spins with unbalanced magnetic moments of the two substructures, giving an overall significant magnetization value [32,33]. Typical ferrimagnetic materials are the iron oxides and ferrites, and among these magnetite, which can be assumed as a Fe-ferrite, whose chemical formula is $Fe_3O_4$, or better $FeO \cdot Fe_2O_3$ distinguishing the two substructures [23]. In analogy to ferromagnetism, even ferrimagnetism presents similar properties and a Curie point [17]. Since ferrimagnetism is a structure-related phenomenon, it should be taken into account also the possible effect induced by the temperature variation on the structural organization. Just to give a clarifying example, Matsuura et al. [34] reported the study of a spinel $MnV_2O_4$ presenting V-octahedral and Mn-tetrahedral sites as substructures. As shown in Fig. 1, the temperature variations caused a variation of the phase crystal structure (from cubic to tetragonal during cooling) and a consequent side-effect on the ferrimagnetic behavior, affecting the magnetic structure from collinear to non-coplanar ordering.

Lastly, superparamagnetism is a particular form of ferro/ferrimagnetism. In detail, when ferro/ferrimagnetic nanoparticles are very small (below 20 nm), they behave as "single-domain". Due to the thermal fluctuations of the environment, nanoparticles can change direction of magnetization with time/temperature fluctuations. In absence of an external magnetic stimulus applied, their magnetization is negligible, whereas in presence of a magnetic field, their response is the self-alignment with the direction of the stimulus (analogously as for paramagnetism) [35] showing a very intense magnetic susceptibility (from here the prefix "super") due to their intrinsic ferromagnetic/ferrimagnetic nature [17].

Other forms of magnetism are diamagnetism (i.e., the capability of oppose to a magnetic field, due to the absence of unpaired electrons) and antiferromagnetism (which is caused by two interpenetrating structures having an equal antialignment of electrons and overall zero magnetization) [27]. Fig. 2 summarizes the main relevant forms of magnetism and their
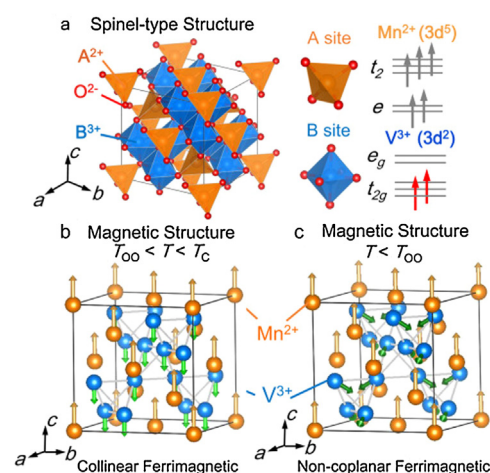


Fig. 1 – Panel a: Crystal structure of the spinel-type oxide $MnV_2O_4$. A-site and B-site ions are surrounded by an oxygen tetrahedron and octahedron, respectively. The $V^{3+}$ ion has orbital degeneracy in the $t_{2g}$ orbital. Panel b: The collinear ferrimagnetic structure between the structural phase transition $T_{OO} = 53$ K and the Curie point $T_c = 58$ K. Panel c: Magnetic structure in the non-coplanar ferrimagnetic tetragonal phase (c < a) below $T_{OO}$. Reprinted with permission from [34].

magnetic behaviors (i.e., superparamagnetism is not reported since merges characteristics of the other forms) [36].

## Magnetic iron oxides synthesis

### Thermodynamics and inter-phase transition

In the last decades, several studies have reported different synthetic routes to produce stable iron oxides nanoparticles (IONPs) characterized by having a certain degree of order in terms of shape and nanoscopic size (namely, with a controlled dimensional dispersity) [37–40].

The magnetic forms of IONPs are basically two: magnetite ($Fe_3O_4$), and its oxidized magnetic form named maghemite ($\gamma$-$Fe_2O_3$) [17]. Since both phases (magnetite and maghemite) present the same crystal organization and magnetite is sensitive to oxidation [37], maghemite is assumed as a ferrous-deficient magnetite, obtained through topotactic oxidation of magnetite's Fe(II) ions into Fe(III) [41,42]. For clarification, Fig. 3 reports the crystal structure of IONPs, namely magnetite, maghemite and hematite [43]. Due to this strict correlation existing between magnetite and maghemite, it is more reasonable to assume both of them being a single magnetite/maghemite phase [44,45].

The most thermodynamically stable form of iron oxides is the fully oxidized hematite ($\alpha$-$Fe_2O_3$), which is an antiferromagnetic (and consequently non-magnetically exploitable) reddish ceramic [46,47], whose crystal structure is reported in Fig. 3a.

By simply heating magnetite under oxidative atmosphere (air), a topotactic oxidation takes place converting magnetite
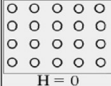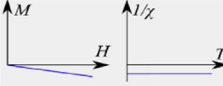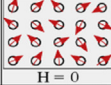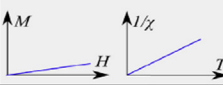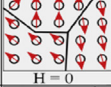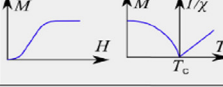
| Magnetism | Examples | Magnetic behaviour | | |
|---|---|---|---|---|
| Diamagnetism | Bi, Si, Cu, inert gases. Susceptibility small and negative ($-10^{-6}$ to $-10^{-5}$) | Atoms have no magnetic moments. H = 0 | $M$ vs $H$ | $1/\chi$ vs $T$ |
| Paramagnetism | Al, $O_2$, MnBi. Susceptibilty small and positive ($10^{-5}$ to $10^{-3}$) | Atoms have randomly oriented magnetic moments. H = 0 | $M$ vs $H$ | $1/\chi$ vs $T$ |
| Ferromagnetism | Fe, Ni, Co, Gd. Susceptibility large (generally > 100) | Atoms are organized in domains which have parallel aligned magnetic moments. H = 0 | $M$ vs $H$ | $M$, $1/\chi$ vs $T$, $T_C$ |
| Antiferromagnetism | Cr, MnO, FeO. Susceptibilty small and positive ($10^{-5}$ to $10^{-3}$) | Atoms are organized in domains which have antiparallel aligned moments. H = 0 | $M$ vs $H$ | $1/\chi$ vs $T$, $T_N$ |
| Ferrimagnetism | $Fe_3O_4$, $MnFe_2O_4$, $NiFe_2O_4$. Susceptibility large (generally > 100) | Atoms are organized in domains which have a mixture of unequal antiparallel aligned moments. H = 0 | $M$ vs $H$ | $M$, $1/\chi$ vs $T$, $T_c$ |

**Fig. 2 – Summary of the main relevant forms of magnetism and their features. Reprinted with permission from [36].**



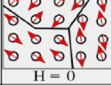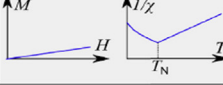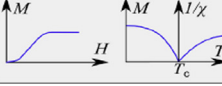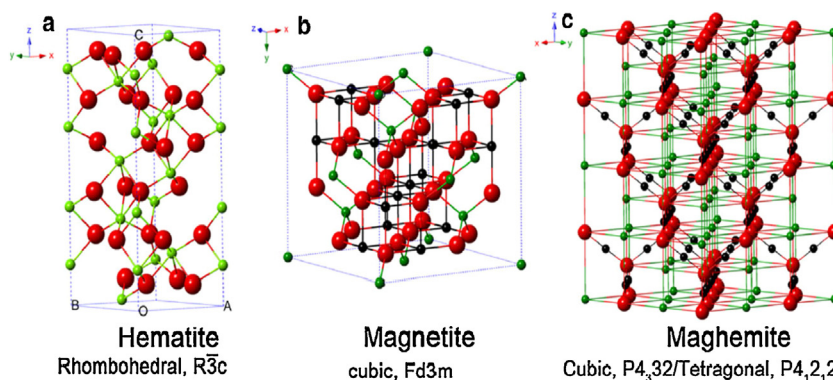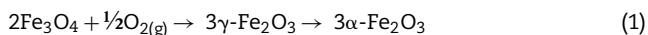**Fig. 3 – Crystal structure and crystallographic data of hematite (a), magnetite (b), and maghemite (c). Legend: Fe(II) (black), Fe(III) (green), and O (red). Reprinted with permission from [43].**

in maghemite and, subsequently (at $T > 600\,^\circ C$), in hematite by phase transformation, as in (1) [48,49].

$$2Fe_3O_4 + \tfrac{1}{2}O_{2(g)} \rightarrow 3\gamma\text{-}Fe_2O_3 \rightarrow 3\alpha\text{-}Fe_2O_3 \qquad (1)$$

On the contrary, when magnetite/maghemite are thermally-treated under a reducing/inert atmosphere and in presence of a carbon source, both oxides reduce themselves into wustite (FeO) and releasing CO as volatile byproduct, through the following reactions (2) and (3) [42,44,48].

$$Fe_3O_4 + C \rightarrow 3FeO + CO_{(g)} \qquad (2)$$

$$\gamma\text{-}Fe_2O_3 + C \rightarrow 2FeO + CO_{(g)} \qquad (3)$$

However, since FeO is thermodynamically unstable above $570\,^\circ C$, it can disproportionate forming elemental iron (Fe-$\alpha$) and magnetite, in a cyclic loop mechanism as in reaction (4).

$$4FeO \rightarrow Fe + Fe_3O_4 \qquad (4)$$

The reactions mechanisms above described confirmed the importance of providing an effective stabilizing coating to preserve magnetite/maghemite IONPs from oxidation (and, consequently, their magnetic response) [17,37]. In particular, from the analysis of the Fe–O phase diagram (Fig. 4), it clearly emerged that at ca. $570\,^\circ C$ different Fe-containing phase may exist, depending on the O-content [50].

The analysis of the literature revealed that several processes might be adopted for the synthesis of magnetic IONPs [37,45]. These methods can be classified according to the source/mechanism as: (i) chemical (co-precipitation, micro-emulsion, sol–gel reactions), (ii) physical (sonochemical, MW-assisted, electrochemical synthesis), (iii) thermal (T-decomposition, spray/laser pyrolysis, hydro/solvothermal), and (iv) biological (bacteria-assisted approaches) processes. In general, the synthesis of IONPs required particular attention in terms of choice of the more convenient experimental conditions able in producing monodisperse distribution of particles, and avoiding/reducing subsequent expensive separation/purification downstream steps, which can dramatically affect the final yield and the industrial feasibility (scale-up) [37,45]. In the following paragraphs the main relevant points
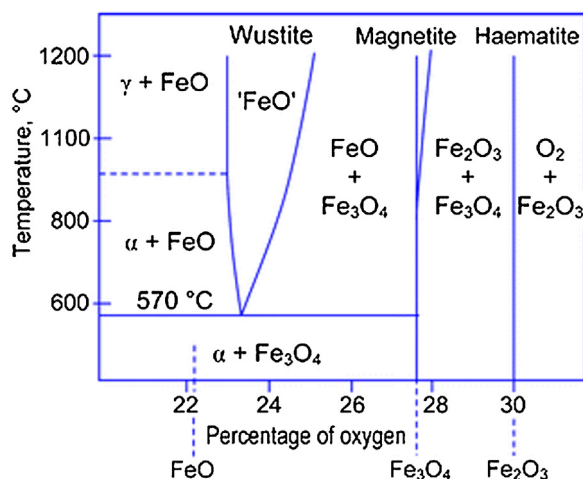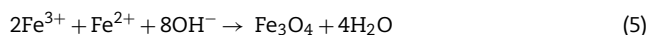
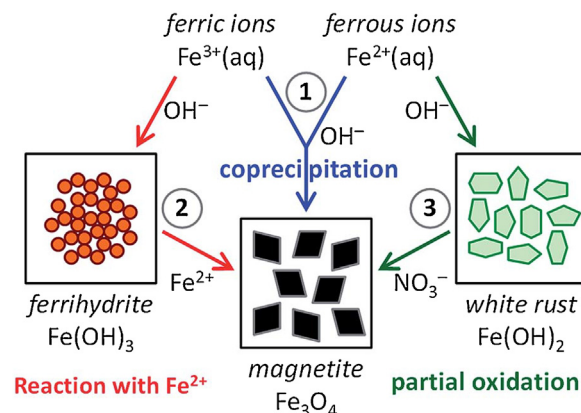Fig. 4 – Fe–O phase diagram. Reprinted with permission from [50].



**Fig. 5 – Schematic representation of the three main chemical routes to obtain magnetite: (1) magnetite formation by controlled co-precipitation from both Fe(II) and Fe(III) ions, (2) magnetite formation from Fe(III) ions through a solid ferrihydrite Fe(OH)$_3$ precursor and Fe(II) ions by ammonia diffusion, and (3) magnetite formation from Fe(II) ions through a solid white rust Fe(OH)$_2$ precursor by partial oxidation with nitrate ions. Reprinted with permission from [51].**

relatively to the different approaches were presented and pros/drawbacks critically discussed.

### Chemical methods

Chemical approaches rely on the growth of magnetic iron oxides (i.e., magnetite) from liquid phase through the action of further chemicals. Among the different approaches, the co-precipitation technique is the simplest and most diffuse pathway exploited for the production of magnetic IONPs [37,39,51]. It consists in the stoichiometric mixture of both ferrous Fe(II) and ferric Fe(III) inorganic salts in presence of a basic environment, following the reaction (5).

$$2Fe^{3+} + Fe^{2+} + 8OH^- \rightarrow Fe_3O_4 + 4H_2O \qquad (5)$$

Since magnetite is poorly soluble in basic environment [52], acidic Fe(II)/Fe(III) when introduced into basic media precipitates as IONPs. According to the literature [53,54], it is possible to drive the synthesis preferentially toward magnetite (rather than maghemite) by working in excess of Fe(II), namely with a Fe(III)/Fe(II) molar ratio <1.75; however, it must be noted that even this precaution can be totally nullified without a stable protection of magnetite surface from the naturally-occurring oxidation. In particular, nucleation is favored at pH < 11, whereas the growth of IONPs at pH > 11 [43]. The co-precipitation route does not require any atmosphere constrains (even if inert atmosphere can be exploited to further control the magnetite's oxidation) [55], the temperature range is very wide (20–250 °C) and the time necessary for the synthesis is relatively low (order of minutes) since pH-mediated [17]. However, these parameters are fundamental for driving both the final size and shape of IONPs, together with the Fe(III)/Fe(II) ratio, ionic strength, stirring rate, and selected Fe-containing salts (i.e., it is well-known the possible role of counterions in influencing the final texture in growing oxides) [43,56–59].

Even if the co-precipitation route is the most widely diffused chemical methods for obtaining IONPs due to the high yields and a certain control in the nanoparticles' size

distribution, this process still presents some limitations, such as the use of non-environmental-friendly chemicals (e.g., strong bases) and the poor shape-control of the final IONPs (i.e., the IONPs growth is kinetically driven). To overcome this issue, in most cases co-precipitation has been integrated with ultrasonic-assisted chemical method, which allows a better control in the nanoparticles' size below 15 nm [60], or by introducing (bio)surfactants and/or stabilizers to confer a further control in sizing/shaping the final IONPs as well as directly-forming a preservative coating (from oxidation) surrounding IONPs [61–65].

Furthermore, the analysis of the co-precipitation process revealed that the magnetite synthesis via co-precipitation is mediated by the preliminary formation of Fe(II)/Fe(III)-hydroxides [66]. Hence, another interesting (alternative) approach found in the literature regards the separation of these two reactions (that in bare co-precipitation reaction happen simultaneously) by mimicking the mineralization process following hydroxide-mediated two-step mechanisms [51]. Fig. 5 resumes these three different pathways, recognizing as route (1) the bare (traditional) co-precipitation process (blue arrows), as route (2) the ferrihydrite-mediated approach (red arrows), and as route (3) the white rust-mediated approach (green arrows) [51].

Considering the ferrihydrite-mediated synthetic line, the selective precipitation of Fe(III) hydroxide is favored by working in a closed system with NH$_3$ vapors diffusing in a Fe(III)/Fe(II) aqueous solution (with Fe(III)/Fe(II) ratio equal to 2) [67,68]. Subsequently, once ferrihydrite Fe(OH)$_3$ precipitates (as in reaction (6)), pH raises to ca. 8, thus evidencing the formation of magnetite (as in reaction (7)) through reaction with the residual Fe(II) ions.

$$Fe^{3+} + 3OH^- \rightarrow Fe(OH)_3 \qquad (6)$$

$$2Fe(OH)_3 + Fe^{2+} + 2OH^- \rightarrow Fe_3O_4 + 4H_2O \qquad (7)$$
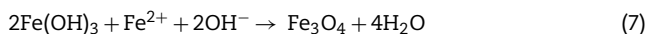
The effectiveness of such ferrihydrite-mediated line is due to a delicate (kinetic) balance between the initial concentration of both Fe-ions and ammonia. These parameters influence also the size and shape of the final IONPs, namely: small/rounded NPs were reached for high [Fe,NH$_3$], whereas large/faceted NPs for low [Fe,NH$_3$] [51].

On the contrary, in the white rust-mediated synthetic line Fe(II) initially precipitates at high pH forming ferrous hydroxide Fe(OH)$_2$ (as in reaction (8)). Subsequently, the hydroxide is oxidized to magnetite by addition of nitrate ions (addition of NO$_3^-$, as in reaction (9)) [51]. Since this process requires an oxidation step, the limiting (kinetic) factor is due to the Fe(II) oxidation rate, which is favored at high pH [69], thus making this synthetic line dependent from the concentration not only of Fe(II)-salt and the base, but also on the oxidant one. Typically, this approach is performed at high temperature (>90 °C) to obtain "single-domain" superparamagnetic IONPs [70].

$$Fe^{2+} + 2OH^- \rightarrow Fe(OH)_2 \qquad (8)$$

$$3Fe(OH)_2 + NO_3^- \rightarrow Fe_3O_4 + NO_2^- + 3H_2O \qquad (9)$$
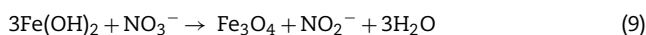
Micro-emulsion processes are based on Fe-containing salts in a water/oil biphasic system, exploiting the presence of amphiphilic (macro)molecules (e.g., surfactants, block-copolymers) at the interface [17]. These amphiphiles consist in hydrophilic head(s) and hydrophobic tail(s) covalently bonded together. Due to their double-nature, these species moved at the interface between the two immiscible phases, self-assembling into supramolecular aggregates of different shapes (e.g., spherical, cylindrical, worm-like, onion-like, lamellar, bi-continuous, and so on) [71–73]. Commonly adopted amphiphiles are cetyltrimethylammonium bromide (CTAB) and polyvinylpyrrolidone (PVP) [74,75]. Hence, the main advantages of micro-emulsions are the narrow size distribution and good shape control on IONPs as both these parameters are influenced by the templating actions induced by amphiphiles species. On the contrary, the main drawback is the aggregation phenomena (IONPs, thus produced, require several post-synthesis purification steps), and the low yield [43].

Lastly, sol–gel routes are based on acid/based-catalyzed hydrolysis/(poly)condensation reactions of precursors (which act as monomers) from colloidal solutions (*sol*) to form a condensed network (*gel*) of metal oxides [76]. For this wet-chemistry approach, precursors adopted are iron alkoxides/salts able to react through hydrolysis/(poly)condensation reactions forming oxides [77,78]. The principal reaction mechanism is based on disproportionation/oxidation/dehydration multi-step reactions (10) [79]:

$$Fe^{3+} + H_2O \cdot Fe(OH)_x{}^{3-x} \rightarrow Fe(OH)_x{}^{3-x} \rightarrow Fe_3O_4 \quad (pH\,9.0,\, 60\,°C)$$
$$(10)$$
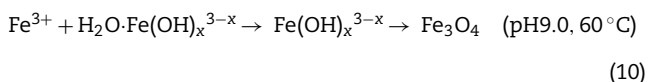
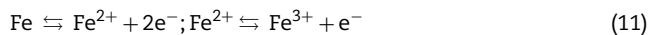For a detailed analysis of the sol–gel processes, please refers to [80]. Interestingly, another possible route alternative to the traditional aqueous sol–gel method is the polyol-mediated approach, which consists in using polyols not only as reaction medium, but also as reducing/stabilizing agents to favor the shape/size control of the growing IONPs [37]. This process is based on dispersing the Fe-containing precursors in liquid polyols (e.g., ethylene glycol), and heating until reaching the boiling point. IONPs obtained via polyols method show hydrophilic surfaces (by the presence of polyol ligands) forming nanoparticles which can be easily-dispersed into polar media. Additionally, high crystallinity IONPs were obtained due to the relatively high reaction temperatures. Conversely, the use of alkoxides as oxidic precursors as well as the alcoholic byproducts released during the calcination step rise the costs/risks of these processes [43].

### Physical methods

Physical methods rely on the exploitation of physical phenomena (e.g., acoustic cavitation, microwave, electrical fields) to induce the growth of magnetite from (non)-aqueous media. The sonochemical approach is based on the sonication of an aqueous ferric/ferrous solution at ambient conditions and in presence of air [17]. Ultrasounds generate alternating expansive/compressive acoustic waves, forming oscillating microbubbles (cavitation phenomenon) [43]. The collapse of these bubbles forms localized hot-spots (with temperature of ca. 4500 °C and pressure of ca. 1000 bar) that can be exploited for the conversion of Fe salts into IONPs [81,82]. This technique is very interesting as obtained IONPs show a very high stability and strong magnetic properties. The main drawbacks of this method is the very low shape control. Additionally, since this process is very fast, amorphous IONPs can also be obtained [79,83].

Microwaves (MW) irradiation, instead, consists in exciting molecules by using an electromagnetic source emitting in the 1–10$^3$ mm wavelength range [17]. When irradiated, molecules aligned themselves with the external field and this motion causes an internal heating [43]. The MW-assisted route causes a reduction of both treatment time and energy consumption, allowing to obtain IONPs from organic solvents, easily dispersible in aqueous medium without any further purification step. As reported by Pascu et al. [84], the production of MW-mediated IONPs generates nanoparticles with low surface reactivity, and this side-effect could be associated to a possible different crystallographic orientation.

Lastly, the electrochemical route consists in a galvanic cell with two electrodes (made by metallic iron) immersed in a saline solution [17]. In this system, several electrochemical reactions take place, namely: the iron electro-oxidation (11) and the water electrolysis (12) at the anode, as well as the water reduction (13) at the cathode.

$$Fe \leftrightarrows Fe^{2+} + 2e^-; Fe^{2+} \leftrightarrows Fe^{3+} + e^- \qquad (11)$$

$$H_2O \leftrightarrows 2H^+ + \tfrac{1}{2}O_{2(g)} + 2e^- \qquad (12)$$

$$2H_2O + 2e^- \leftrightarrows H_{2(g)} + 2OH^- \qquad (13)$$

Subsequently, the pH moves from acid to basic, causing the precipitation of Fe(III) hydroxides, following reaction (14):

$$Fe^{3+} + 3OH^- \leftrightarrows Fe(OH)_3 \qquad (14)$$

Fe(III) hydroxide can evolve into two different mechanisms, according to the solution's pH: (i) either toward hematite or goethite through dehydration (pH < 8), or (ii) directly to the magnetic magnetite (pH > 8–9), as in reaction (15).

$$3Fe(OH)_3 + H^+ + e^- \leftrightarrows Fe_3O_4 + 5H_2O \qquad (15)$$
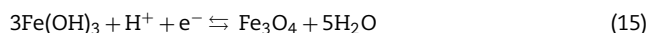
Parameters influencing the electrochemical reaction pathways are pH, temperature, and reaction time, as well as the working distance between electrodes. In particular, this last point is crucial since only distances below 5 cm are able to favor the desired pH environment at the cathode (and, consequently, the magnetite growth). This method has many advantages, one above all the capability of controlling the IONPs particle size (by varying electrical parameters) characterized by having hydrophilic surfaces [85].

### Thermal methods

Thermal methods rely on the exploitation of higher temperature processes respect to the others to obtain iron oxide nanomaterials from inorganic salts (even in absence of solvents) [17]. The most diffuse one is the thermal decomposition from non-aqueous mixture of Fe-containing salts into a closed vessel under inert atmosphere [17,37,86]. As reported by Wu and co-workers [43], thermal decomposition strategies can be classified as either conventional (where precursors are heated) or hot-injection approaches (where precursors are injected into a hot reaction mixture). The main advantage of these processes is the high crystallinity degree of IONPs (due to the high temperatures reached within these processes). Furthermore, a well-defined size and shape control can be exerted by introducing specific stabilizers into the reaction medium, which exert a certain control (reducing) the rate of IONPs formation [17]. This technique is very powerful for obtaining particular morphologies (e.g., nanocubes, core-shell systems, and so on) [87]. One characteristic of the IONPs produced following this procedure is the presence of hydrophobic surfaces that favor their dissolution into apolar solvents. Other thermal approaches are the spray/laser pyrolysis and the hydro/solvo-thermal routes.

Spray pyrolysis consists in producing IONPs via spray-drying process of Fe(III) salts-containing organic solvents drops and, subsequent, pyrolysis. Parameters influencing the IONPs particles' size are both drop size and the evaporation rate of solvents [88]. Laser pyrolysis, instead, uses a laser source for heating a gaseous mixture of Fe(III) salts-containing precursors in a (inert) gas carrier [89].

Hydro- and solvo-thermal routes are based on crystallization reactions happening into sealed containers (i.e., autoclave) at temperatures in the 150–250 °C range and pressure (3–40 bar) [43]. The IONPs production is driven by dehydration reaction of inorganic salts (precursors) and by the low solubility of the resulting oxides, which supersaturate the medium [79]. Hydrothermal processes are usually selected for magnetite production, whereas maghemite requires a certain degree of oxidation (mostly it is obtained through solvothermal routes) [90]. Even these processes allow obtaining high crystalline IONPs due to the temperature reached. Additionally, a very high shape control can be obtained by simply varying the initial concentration of Fe-precursor and the time/temperature of the treatment [17].

In general, all thermal methods allow reaching high conversion yields, thus making these IONPs production processes very attractive since industrially scalable.

### Biological methods

Biological methods consist in the exploitation of microbial species (mainly bacteria) to convert Fe-ions into IONPs by means of biological processes. Magnetotactic bacteria are a group of Gram-negative prokaryotes that are sensible to the geomagnetic field by means of the presence of magnetosomes, which are intracellular structures containing magnetic magnetite or greigite ($Fe_3S_4$) [91,92]. These bacterial magnetosomes are usually in the 35–120 nm range, and magnetic IONPs formed are uniformly "single-domain" (superparamagnetic) permanently magnetic at RT, even without applying an external magnetic field [93].

Studies reported that different oxides morphologies can be reached, typically cubo-octahedral, bullet-shaped, elongated prismatic and rectangular one (see for instance the morphologies in Fig. 6) [17,91]. Since being biological, the exact mechanism of the IONPs formation within the magnetosomes is very complex. Probably it includes different steps, such as the vesicles formation, the extracellular Fe uptake by the microorganism and the biomineralization of magnetite/greigite within the magnetosomes [91,92,94]. Just to provide an example, the hypothetical model for magnetosome biosynthesis in a magnetotactic bacterium is reported in Fig. 7 [91].

Interestingly, Curcio and co-workers [95] proposed an alternative cyclic method where intracellular magnetosomes can experience an important biodegradation associated with the progressive magnetite-to-ferrihydrite phase transition, and subsequently identified that ionic species delivered by this degradation could be used by cells to biosynthesize magnetite nanoparticles.

In general, biological methods are green/sustainable processes, very appealing since favor the direct production of IONPs that exhibit high biocompatibility. As reported by Araujo et al. [96], the direct use of magnetosomes is very interesting since they show relatively specific magnetic and crystalline properties together with an enveloping biological membrane (not observed in abiotically produced IONPs) that make them of great interest for biotechnology applications. The main drawback of these biosynthetic routes is the relatively difficulty in controlling both size and shape of IONPs [43]. Additionally, since these processes exploit the catalyzing action of living microorganisms (which are sensible to many factors), biological routes allow obtaining low yields of IONPs, limiting their effective applications.
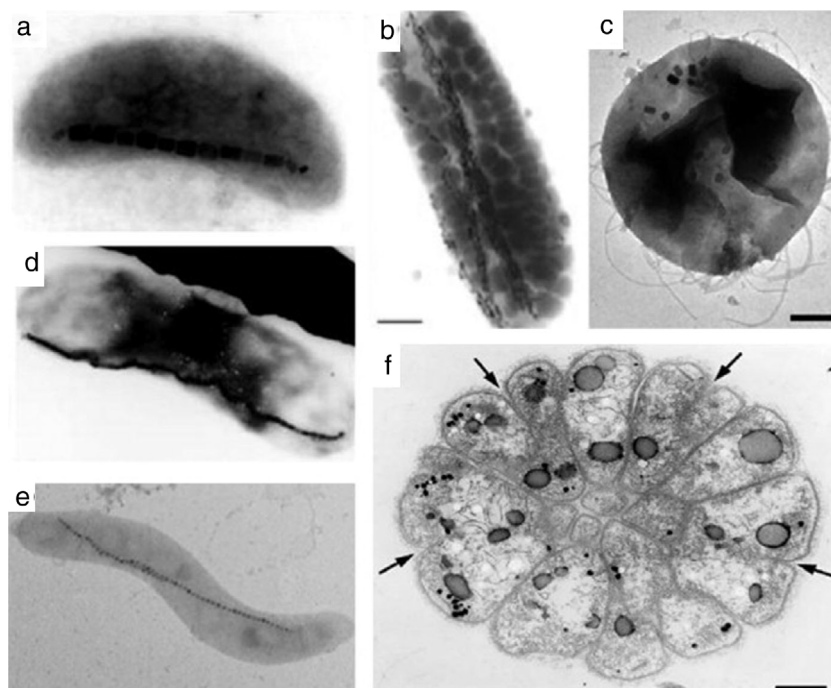
**Fig. 6 – Various morphology of magnetotactic bacteria: (a) vibrios, (b, d) rods (b marker = 1 µm), (c) coccoid (c marker = 200 nm), (e) spirilla, and (f) multicellular organism (f marker = 1 µm). Black nanostructures in micrographs are IONPs. Reprinted with permission from [91].**
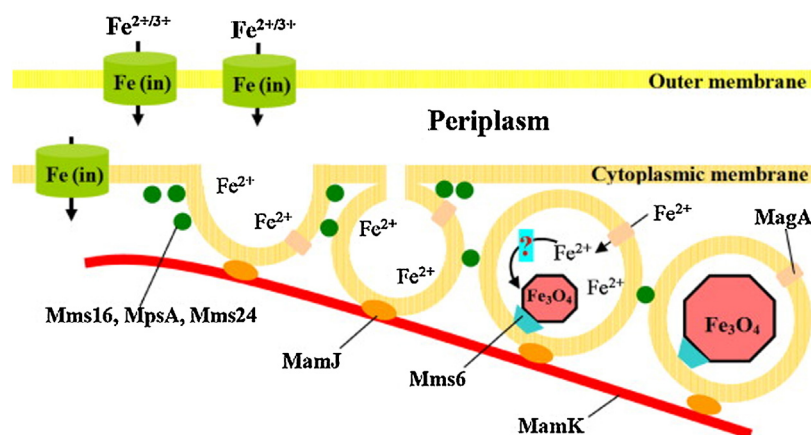


**Fig. 7 – Scheme of the hypothesized mechanism of magnetite biomineralization. Reprinted with permission from [91].**

*Critical remarks*

A comparison between the different synthetic methods is summarized in Table 1. The analysis of the different methods allows to highlight the following "gold" rules:

- Chemical methods: these processes are made under air atmosphere, in a range of temperature going from RT to 250 °C, and allow obtaining a nanoparticles' size distribution narrow, and a good shape control (the only exception is the co-precipitation route).
- Physical methods: these processes are made under air atmosphere, at low temperature (the only exception is the MW-assisted route), obtaining a medium size distribution

and medium yields. Depending on the method, it is possible to reach even a high shape control.
- Thermal methods: these processes require particular attention concerning the atmosphere (usually required inert gases and/or high pressure) and high temperature of reactions. These particularly hard synthetic conditions allow obtaining high yields of IONPs, characterized by having a very narrow size distribution and a good shape control.
- Biological methods: these processes require very mild conditions (in terms of reaction environment and temperatures). Due to the presence of living microorganisms, the final yields of conversion are very low, with a poor size/shape control of the resulting IONPs.

**Table 1 – Classification of the synthetic routes for the production of IONPs.**

| Methods | Atmosphere | Temperature (°C) | Time | IONPs size distribution | IONPs shape control | IONPs yield |
|---------|-----------|------------------|------|------------------------|---------------------|-------------|
| Co-precipitation | Ambient | 20–250 | min | Narrow | (Not) good | High |
| Micro-emulsion | Ambient | 20–80 | h | Narrow | Good | Low |
| Sol–gel | Ambient | 25–200 | h | Narrow | Good | Medium |
| Sonochemical | Ambient | 20–50 | min | Narrow | Bad | Medium |
| MW-assisted | Ambient | 100–200 | min | Medium | Good | Medium |
| Electrochemical | Ambient | 20–30 | h/days | Medium | Medium | Medium |
| T-decomposition | Inert | 100–350 | h/days | Very narrow | Very good | High |
| Spray/laser pyrolysis | Inert | >100 | min/h | Narrow | Medium | High |
| Hydro/solvothermal | High pressure | 150–220 | h/days | Very narrow | Very good | High |
| Bacteria-assisted | Ambient | 20–30 | h/days | Broad | Bad | Low |

By focusing on the industrial feasibility, the more performing processes are the ones showing high conversion yields (namely, co-precipitation and the thermal methods). Among these ones, the co-precipitation (chemical) method is surely the most diffuse since it requires mild conditions compared to the thermal methods. On the contrary, the main limitation of this approach is the poor shape control. For this reason, several methods were adopted for better the size and shape control in IONPs obtained through co-precipitation method, such as the use of structure directing agents. These "growing factors" can be either nucleating agents (i.e., seeds) able in favoring the formation of particular shapes (e.g., metastable structures) [97,98] or amphiphiles able in driving the preferential growth of specific crystal surfaces [74,75]. Thermal methods, instead, guarantee from one side a very strict morphological control, but on the other side all of them require hard synthetic conditions.

## Conclusions

In the last decades, a great interest has risen up on magnetic ceramics. Among this category of materials, iron oxides represent one of the most studied and performing family of ceramics that still today guarantees the best compromise between costs and magnetic performances. Even if iron oxides are naturally occurring substrates, several synthetic protocols were exploited to successfully obtain nanostructures with a high morphological (i.e., size and shape) control. With this review, the main relevant synthetic protocols found in the literature for obtaining specific magnetic phases with controlled geometries and dimensions were critically discussed.

In detail, the different types of magnetisms as well as the iron oxide crystal phases were presented, together with the main chemical/physical/thermal/biological synthetic methods. In this context, the main focus of this document relies on highlighting the (dis)advantages of the different methods in terms of morphology control degree in the resulting products. Among the different methods here summarized, co-precipitation chemical route and the thermal methods represent the more performing processes in term of industrial feasibility and final yields. Lastly, rather than focusing on every possible case study findable in the literature, the main relevant features of each process were critically discussed, and the main relevant guidelines pointed out.

## REFERENCES

[1] R. Pampuch, A brief history of ceramic innovation, in: R. Pampuch (Ed.), An Introduction to Ceramics Lecture Notes in Chemistry, 86, Springer, Cham, Switzerland, 2014, ISBN 978-3-319-10409-6, pp. 1–17, http://dx.doi.org/10.1007/978-3-319-10410-2_1.

[2] J. de Juan Ares, N. Schibille, La Hispania antigua y medieval a través del vidrio: la aportación de la arqueometría, Bol. Soc. Españ. Cerám. Vidrio 56 (2017) 195–204, http://dx.doi.org/10.1016/j.bsecv.2017.04.001.

[3] V. Cannavò, A. Cardarelli, S. Lugli, G. Vezzalini, S.T. Levi, Fabrics and archaeological facies in northern Italy: an integrated approach to technological and stylistic choices in Bronze Age pottery production, J. Archaeol. Sci. Rep. 16 (2017) 521–531, http://dx.doi.org/10.1016/j.jasrep.2017.03.016.

[4] L. Maritan, L. Nodari, C. Mazzoli, A. Milano, U. Russo, Influence of firing conditions on ceramic products: Experimental study on clay rich in organic matter, Appl. Clay Sci. 31 (2006) 1–15, http://dx.doi.org/10.1016/j.clay.2005.08.007.

[5] R. Nisticò, The importance of surfaces and interfaces in clays for water remediation processes, Surf. Topogr.: Metrol. Prop. 6 (2018) 043001, http://dx.doi.org/10.1088/2051-672X/aaed09.

[6] R. Nisticò, L. Lavagna, D. Versaci, P. Benzi, Chitsan and its char as fillers in cement-base composites: a case study, Bol. Soc. Españ. Cerám. Vidrio (2019), http://dx.doi.org/10.1016/j.bsecv.2019.10.002 (in press).

[7] M. Manzano, M. Vallet-Regi, Revisiting bioceramics: bone regenerative and local drug delivery systems, Prog. Solid State Chem. 40 (2012) 17–30, http://dx.doi.org/10.1016/j.progsolidstchem.2012.05.001.

[8] G. Varghese, M. Moral, M. Castro-Garcia, J.J. Lopez-Lopez, J.R. Marin-Rueda, V. Tague-Alcaraz, L. Hernandez-Afonso, J.C. Ruiz-Morales, J. Canales-Vazquez, Fabrication and characterisation of ceramics via low-cost DLP 3D printing, Bol. Soc. Españ. Cerám. Vidrio 57 (2018) 9–18, http://dx.doi.org/10.1016/j.bsecv.2017.09.004.

[9] T.A. Blank, L.P. Eksperiandova, K.N. Belikov, Recent trends of ceramic humidity sensors development: a review, Sensors Actuators B: Chem. 228 (2016) 416–442, http://dx.doi.org/10.1016/j.snb.2016.01.015.

[10] K.N. Dinh, Q. Liang, C.-F. Du, J. Zhao, A.I.Y. Tok, H. Mao, Q. Yan, Nanostructured metallic transition metal carbides, nitrides, phosphides, and borides for energy storage and conversion, Nano Today 25 (2019) 99–121, http://dx.doi.org/10.1016/j.nantod.2019.02.008.

[11] M.C. Tanzi, S. Farè, G. Candiani, Chapter 1 – Organization structure, and properties of materials, in: M.C. Tanzi, S. Farè, G. Candiani (Eds.), Foundations of Biomaterials Engineering, 1st ed., Academic Press, London, UK, 2019, ISBN

978-0-08-101034-1, pp. 3–103,
http://dx.doi.org/10.1016/B978-0-08-101034-1.00001-3.

[12] H. Shokrollahi, A review of the magnetic properties, synthesis methods and applications of maghemite, J. Magn. Magn. Mater. 426 (2017) 74–81, http://dx.doi.org/10.1016/j.jmmm.2016.11.033.

[13] MicromarketMonitor.com. Europe permanent magnet market. Available at: http://www.micromarketmonitor.com/market/europe-permanent-magnet-7897577725.html (accessed 21.11.19).

[14] L.J. Money, The saga of MAGLEV, Transp. Res. Part A: Gen. 18 (1984) 333–341, http://dx.doi.org/10.1016/0191-2607(84)90171-7.

[15] M. McLean, S. Engstrom, R. Honeycomb, Static magnetic fields for the treatment of pain, Epilep. Behav. 2 (2001) S74–S80, http://dx.doi.org/10.1006/ebeh.2001.0211.

[16] R.M. Bozorth, Magnetism, Rev. Mod. Phys. 19 (1947) 29–86, doi:10.1103/RevModPhys.19.29.

[17] R. Nisticò, Magnetic materials and water treatments for a sustainable future, Res. Chem. Intermed. 43 (2017) 6911–6949, http://dx.doi.org/10.1007/s11164-017-3029-x.

[18] H.C. Oersted, Experiments on the effect of a current of electricity on the magnetic needles, Ann. Philos. 16 (1820) 273–277.

[19] M. Faraday, V. Experimental researches in electricity, Philos. Trans. R. Soc. London 122 (1832) 125–162, http://dx.doi.org/10.1098/rstl.1832.0006.

[20] P. Quarterman, C. Sun, J. Garcìa-Barriocanal, D.C. Mehedra, Y. Lv, S. Manipatruni, D.E. Nikonov, I.A. Young, P.M. Voyles, J.-P. Wang, Demonstration of Ru as the 4th ferromagnetic element at room temperature, Nat. Commun. 9 (2018) 2058, http://dx.doi.org/10.1038/s41467-018-04512-1.

[21] C. Clausell, A. Barba, Processing–microstructure–properties relationship in a CuNiZn ferrite, Bol. Soc. Españ. Cerám. Vidrio 57 (2018) 29–39, http://dx.doi.org/10.1016/j.bsecv.2017.09.002.

[22] A.G. Roca, L. Gutierrez, H. Gavilan, M.E. Fortes Brollo, S. Veintemillas-Verdaguer, M. del Puerto Morales, Design strategies for shape-controlled magnetic iron oxide nanoparticles, Adv. Drug Deliv. Rev. 138 (2019) 68–104, http://dx.doi.org/10.1016/j.addr.2018.12.008.

[23] D.H.K. Reddy, Y.-S. Yun, Spinel ferrite magnetic adsorbents: alternative future materials for water purification? Coord. Chem. Rev. 315 (2016) 90–111, http://dx.doi.org/10.1016/j.ccr.2016.01.012.

[24] C.M.B. Henderson, J.M. Charnock, D.A. Plant, Cation occupancies in Mg Co, Ni, Zn, Al ferrite spinels: a multi-element EXAFS study, J. Phys.: Condens. Matter 19 (2017) 076214, http://dx.doi.org/10.1088/0953-8984/19/7/076214.

[25] B.B. Manshian, U. Himmerlreich, S.J. Soenen, Impact of core and functionalized magnetic nanoparticles on human health, in: N.T.K. Thanh (Ed.), Clinical Applications of Magnetic Nanoparticles, CRC Press/Taylor and Francis Group, Boca Raton, USA, 2018, ISBN 978-1-138-05155-3, pp. 289–304 (chapter 15).

[26] R.M. Cornell, U. Schwertmann, The Iron Oxides: Structure, Properties, Reactions Occurrences and Uses, 2nd ed., Wiley-VCH, Weinheim (Germany), 2013, ISBN 978-3527302741, http://dx.doi.org/10.1002/3527602097.

[27] R. Nisticò, F. Cesano, F. Garello, Magnetic materials and systems: domain structure visualization and other characterization techniques for the application in the materials science and biomedicine, Inorganics 8 (2020) 6, doi:10.3390/inorganics8010006.

[28] G. Gerstein, V.A. L'vov, A. Zak, W. Dudzinski, H.J. Maier, Direct observation of nano-dimensional internal structure of ferromagnetic domains in the ferromagnetic shape memory alloy Co–Ni–Ga, J. Magn. Magn. Mater. 466 (2018) 125–129, http://dx.doi.org/10.1016/j.jmmm.2018.06.066.

[29] J.M.D. Coey, Magnetism in future, J. Magn. Magn. Mater. 226–230 (2001) 2107–2112, http://dx.doi.org/10.1016/S0304-8853(01)00023-3.

[30] R.D. James, Materials science: magnetic alloys break the rules, Nature 521 (2015) 298–299, http://dx.doi.org/10.1038/521298a.

[31] K. Ando, Seeking room-temperature ferromagnetic semiconductors, Science 312 (2006) 1883–1885, doi:10.1126/science.1125461.

[32] E.C. Devi, I. Soibam, Tuning the magnetic properties of a ferrimagnet, J. Magn. Magn. Mater. 469 (2019) 587–592, http://dx.doi.org/10.1016/j.jmmm.2018.09.034.

[33] R.C. Pullar, Hexagonal ferrites: a review of the synthesis, properties and applications of hexaferrite ceramics, Prog. Mater. Sci. 57 (2012) 1191–1334, http://dx.doi.org/10.1016/j.pmatsci.2012.04.001.

[34] K. Matsuura, H. Sagayama, A. Uehara, Y. Nii, R. Kajimoto, K. Kamazawa, K. Ikeuchi, S. Ji, N. Abe, T. Arima, Magnetic excitations in the orbital disordered phase of $MnV_2O_4$, Physica B: Condens. Matter 536 (2018) 372–376, http://dx.doi.org/10.1016/j.physb.2017.09.085.

[35] J. Liu, Z. Wu, Q. Tian, W. Wu, X. Xiao, Shape-controlled iron oxide nanocrystals: synthesis, magnetic properties and energy conversion applications, CrystEngComm 18 (2016) 6303–6326, http://dx.doi.org/10.1039/C6CE01307D.

[36] S. Palagummi, F.-G.8 Yuan, Magnetic levitation and its application for low frequency vibration energy harvesting, in: F.-G. Yuan (Ed.), Structural Health Monitoring (SHM) in Aerospace Structures, Woodhead Publishing Series in Composites Science and Engineering, Amsterdam Netherlands, 2016, pp. 213–251, http://dx.doi.org/10.1016/B978-0-08-100148-6.00008-1.

[37] S. Laurent, D. Forge, M. Port, A. Roch, C. Robic, L.V. Elst, R.N. Muller, Magnetic iron oxide nanoparticles: Synthesis, stabilization, vectorization, physicochemical characterizations, and biological applications, Chem. Rev. 108 (2008) 2064–2110, http://dx.doi.org/10.1021/cr068445e.

[38] D. Stanicki, L.V. Elst, R.N. Muller, S. Laurent, Synthesis and processing of magnetic nanoparticles, Curr. Opin. Chem. Eng. 8 (2015) 7–14, http://dx.doi.org/10.1016/j.coche.2015.01.003.

[39] Y.L. Pang, S. Lim, H.C. Ong, W.T. Chong, Research progress on iron oxide-based magnetic materials: synthesis techniques and photocatalytic applications, Ceram. Int. 42 (2016) 9–34, http://dx.doi.org/10.1016/j.ceramint.2015.08.144.

[40] D. Ling, T. Hyeon, Chemical design of biocompatible iron oxide nanoparticles for medical applications, Small 9 (2013) 1450–1466, http://dx.doi.org/10.1002/smll.201202111.

[41] R. Dronskowski, The little maghemite story: a classical functional material, Adv. Funct. Mater. 11 (2001) 27–29, doi: 10.1002/1616-3028(200102)11:1<27::AID-ADFM27>3.0.CO; 2-X.

[42] F. Cesano, G. Fenoglio, L. Carlos, R. Nisticò, One-step synthesis of magnetic chitosan polymer composite films, Appl. Surf. Sci. 345 (2015) 175–181, http://dx.doi.org/10.1016/j.apsusc.2015.03.154.

[43] W. Wu, Z. Wu, T. Yu, C. Jiang, W.-S. Kim, Recent progress on magnetic iron oxide nanoparticles: synthesis, surface functional strategies and biomedical applications, Sci. Technol. Adv. Mater. 16 (2015) 023501, http://dx.doi.org/10.1088/1468-6996/16/2/023501.

[44] R. Nisticò, F. Franzoso, F. Cesano, D. Scarano, G. Magnacca, M.E. Parolo, L. Carlos, Chitosan-derived iron oxide systems for magnetically guided and efficient water purification processes from polycyclic aromatic hydrocarbons, ACS Sustain. Chem. Eng. 5 (2017) 793–801, http://dx.doi.org/10.1021/acssuschemeng.6b02126.

[45] A. Bianco Prevot, A. Arques, L. Carlos, E. Laurenti, G. Magnacca, R. Nisticò, Chapter 7 – Innovative sustainable materials for the photoinduced remediation of polluted water, in: C.M. Galanakis, E. Agrafioti (Eds.), Sustainable Water and Wastewater Processes, Elsevier Inc., Amsterdam, Netherlands, 2019, ISBN 978-0-12-816170-8, pp. 203–238, http://dx.doi.org/10.1016/B978-0-12-816170-8.00007-7.

[46] J. Jacob, M.A. Khadar, VSM and Mössbauer study of nanostructured hematite, J. Magn. Magn. Mater. 322 (2010) 614–621, http://dx.doi.org/10.1016/j.jmmm.2009.10.025.

[47] L. Demarchis, M. Minella, R. Nisticò, V. Maurino, C. Minero, D. Vione, Photo-Fenton reaction in the presence of morphologically controlled hematite as iron source, J. Photochem. Photobiol. A: Chem. 307 (2015) 99–107, http://dx.doi.org/10.1016/j.jphotochem.2015.04.009.

[48] E.R. Monazam, R.W. Breault, R. Siriwardane, Kinetics of magnetite ($Fe_3O_4$) oxidation to hematite ($Fe_2O_3$) in air for chemical looping combustion, Ind. Eng. Chem. Res. 53 (2014) 13320–13328, http://dx.doi.org/10.1021/ie501536s.

[49] R. Nisticò, F. Cesano, F. Franzoso, G. Magnacca, D. Scarano, I.G. Funes, L. Carlos, M.E. Parolo, From biowaste to magnet-responsive materials for water remediation from polycyclic aromatic hydrocarbons, Chemosphere 202 (2018) 686–693, http://dx.doi.org/10.1016/j.chemosphere.2018.03.153.

[50] K. Ostrikov, I. Levchenko, U. Cvelbar, M. Sunkara, M. Mozetic, From nucleation to nanowires: a single-step process in reactive plasmas, Nanoscale 2 (2010) 2012–2027, http://dx.doi.org/10.1039/c0nr00366b.

[51] J.J.M. Lenders, G. Mirabello, N.A.J.M. Sommerdijk, Bioinspired magnetite synthesis via solid precursor phases, Chem. Sci. 7 (2016) 5624–5634, http://dx.doi.org/10.1039/c6sc00523c.

[52] S.E. Ziemniak, M.E. Jones, K.E.S. Combs, Magnetite solubility and phase stability in alkaline media at elevated temperatures, J. Sol. Chem. 24 (1995) 837–877, http://dx.doi.org/10.1007/BF00973442.

[53] W. Jiang, K.-L. Lai, H. Hu, X.-B. Zeng, F. Lang, K.-X. Liu, Y. Wu, Z.-W. Gu, The effect of $[Fe^{3+}]/[Fe^{2+}]$ molar ratio and iron salts concentration on the properties of superparamagnetic iron oxide nanoparticles in the water/ethanol/toluene system, J. Nanopart. Res. 13 (2011) 5135–5145, http://dx.doi.org/10.1007/s11051-011-0495-8.

[54] F. Franzoso, R. Nisticò, F. Cesano, I. Corazzari, F. Turci, D. Scarano, A. Bianco Prevot, G. Magnacca, L. Carlos, D.O. Martire, Biowaste-derived substances as a tool for obtaining magnet-sensitive materials for environmental applications in wastewater treatments, Chem. Eng. J. 310 (2017) 307–316, http://dx.doi.org/10.1016/j.cej.2016.10.120.

[55] T. Ahn, J.H. Kim, H.-M. Yang, J.W. Lee, J.-D. Kim, Formation pathways of magnetite nanoparticles by coprecipitation method, J. Phys. Chem. C 116 (2012) 6069–6076, http://dx.doi.org/10.1021/jp211843g.

[56] F. Yazdani, M. Seddigh, Magnetite nanoparticles synthesized by co-precipitation method: the effects of various iron anions on specifications, Mater. Chem. Phys. 184 (2016) 318–323, http://dx.doi.org/10.1016/j.matchemphys.2016.09.058.

[57] R. Nisticò, G. Magnacca, M. Antonietti, N. Fechler, "Salted silica": Sol–gel chemistry of silica under hypersaline conditions, Zeitsc. Anorgan. Allgem. Chem. 640 (2014) 582–587, http://dx.doi.org/10.1002/zaac.201300526.

[58] R. Nisticò, G. Magnacca, The hypersaline synthesis of titania: from powders to aerogels, RSC Adv. 5 (2015) 14333–14340, http://dx.doi.org/10.1039/c4ra13573c.

[59] R. Nisticò, S. Tabasso, G. Magnacca, T. Jordan, M. Shalom, N. Fechler, Reactive hypersaline route: one-pot synthesis of porous photoreactive nanocomposites, Langmuir 33 (2017) 5213–5222, http://dx.doi.org/10.1021/acs.langmuir.7b00142.

[60] S. Wu, A.Z. Sun, F.Q. Zhai, J. Wang, W.H. Xu, Q. Zhang, A.A. Volinsky, $Fe_3O_4$ magnetic nanoparticles synthesis from tailings by ultrasonic chemical co-precipitation, Mater. Lett. 65 (2011) 1882–1884, http://dx.doi.org/10.1016/j.matlet.2011.03.065.

[61] K. Petcharoen, A. Sirivat, Synthesis and characterization of magnetite nanoparticles via the chemical co-precipitation method, Mater. Sci. Eng. B 177 (2012) 421–427, http://dx.doi.org/10.1016/j.mseb.2012.01.003.

[62] H. Pardoe, W. Chua-anusorn, T.G. St. Pierre, J. Dobson, Structural and magnetic properties of nanoscale iron oxide particles synthesized in the presence of dextran or polyvinyl alcohol, J. Magn. Magn. Mater. 225 (2001) 41–46, http://dx.doi.org/10.1016/S0304-8853(00)01226-9.

[63] D. Palma, A. Bianco Prevot, M. Brigante, D. Fabbri, G. Magnacca, C. Richard, G. Mailhot, R. Nisticò, New insights on the photodegradation of caffeine in the presence of bio-based substances-magnetic iron oxide hybrid nanomaterials, Materials 11 (2018) 1084, doi:10.3390/ma11071084.

[64] L. Shen, Y. Qiao, Y. Guo, S. Meng, G. Yang, M. Wu, J. Zhao, Facile co-precipitation synthesis of shape-controlled magnetite nanoparticles, Ceram. Int. 40 (2014) 1519–1524, http://dx.doi.org/10.1016/j.ceramint.2013.07.037.

[65] A. Bianco Prevot, F. Baino, D. Fabbri, F. Franzoso, G. Magnacca, R. Nisticò, A. Arques, Urban biowaste-derived sensitizing materials or caffeine photodegradation, Environ. Sci. Pollut. Res. 24 (2017) 12599–12607, http://dx.doi.org/10.1007/s11356-016-7763-1.

[66] J.P. Jolivet, C. Chaneac, E. Tronc, Iron oxide chemistry. From molecular clusters to extended solid networks, Chem. Commun. 10 (2004) 481–487, http://dx.doi.org/10.1039/B304532N.

[67] J. Baumgartner, A. Dey, P.H.H. Bomans, C. Le Coadou, P. Fratzl, N.A.J.M. Sommerdijk, D. Faivre, Nucleation and growth of magnetite from solution, Nat. Mater. 12 (2013) 310–314, http://dx.doi.org/10.1038/nmat3558.

[68] J. Baumgartner, M.A. Carillo, K.M. Eckes, P. Werner, D. Faivre, Biomimetic magnetite formation: from biocombinatorial approaches to mineralization effects, Langmuir 30 (2014) 2129–2136, http://dx.doi.org/10.1021/la404290c.

[69] F. Vereda, J. de Vicente, R. Hidalgo-Alvarez, Oxidation of ferrous hydroxides with nitrate: a versatile method for the preparation of magnetic colloidal particles, J. Colloid Interface Sci. 392 (2013) 50–56, http://dx.doi.org/10.1016/j.jcis.2012.09.064.

[70] C.L. Altan, J.J.M. Lenders, P.H.H. Bomans, G. de With, H. Friedrich, S. Bucak, N.A.J.M. Sommerdijk, Partial oxidation as a rational approach to kinetic control in bioinspired magnetite synthesis, Chem. – Eur. J. 21 (2015) 6150–6156, http://dx.doi.org/10.1002/chem.201405973.

[71] C. Solans, M.J. Garcia-Celma, Surfactants for microemulsions, Curr. Opin. Colloid Interface Sci. 2 (1997) 464–471, http://dx.doi.org/10.1016/S1359-0294(97)80093-3.

[72] R. Nisticò, Block copolymers for designing nanostructured porous coatings, Beilstein J. Nanotechnol. 9 (2018) 2332–2344, http://dx.doi.org/10.3762/bjnano.9.218.

[73] R. Nisticò, P. Avetta, P. Calza, D. Fabbri, G. Magnacca, D. Scalarone, Selective porous gates made from colloidal silica nanoparticles, Beilstein J. Nanotechnol. 6 (2015) 2105–2112, doi:10.3762/bjnano.6.215.

[74] T. Lu, J. Wang, J. Yin, A. Wang, X. Wang, T. Zhang, Surfactant effects on the microstructures of $Fe_3O_4$ nanoparticles synthesized by microemulsion method, Colloids Surf. A: Physicochem. Eng. Aspects 436 (2013) 675–683, http://dx.doi.org/10.1016/j.colsurfa.2013.08.004.

[75] R.G. Lopez, M.G. Pineda, G. Hurtado, R.D. de Leon, S. Fernandez, H. Saade, D. Bueno, Chitosan-coated magnetic

nanoparticles prepared in one step by reverse microemulsion precipitation, Int. J. Mol. Sci. 14 (2013) 19636–19650, doi:10.3390/ijms141019636.

[76] R. Nisticò, D. Scalarone, G. Magnacca, Sol–gel chemistry, templating and spin-coating deposition: a combined approach to control in a simple way the porosity of inorganic thin films/coatings, Microporous Mesoporous Mater. 248 (2017) 18–29, http://dx.doi.org/10.1016/j.micromeso.2017.04.017.

[77] O.M. Lemine, K. Omri, B. Zhang, L. El Mir, M. Sajieddine, A. Alyamani, M. Bououdina, Sol–gel synthesis of 8 nm magnetite ($Fe_3O_4$) nanoparticles and their magnetic properties, Superlatt. Microstruct. 52 (2012) 793–799, http://dx.doi.org/10.1016/j.spmi.2012.07.009.

[78] Y.-H. Deng, C.-C. Wang, J.-H. Hu, W.-L. Yang, S.-K. Fu, Investigation of formation of silica-coated magnetite nanoparticles via sol–gel approach, Colloids Surf. A: Physicochem. Eng. Aspects 262 (2005) 87–93, http://dx.doi.org/10.1016/j.colsurfa.2005.04.009.

[79] A. Ali, H. Zafar, M. Zia, I. Haq, A.R. Phull, J.S. Ali, A. Hussain, Synthesis, characterization, applications, and challenges of iron oxide nanoparticles, Nanotechnol. Sci. Appl. 9 (2016) 49–67, doi:10.2147/NSA.S99986.

[80] A.E. Danks, S.R. Hall, Z. Schnepp, The evolution of 'sol–gel' chemistry as a technique for materials synthesis, Mater. Horizons 3 (2016) 91–112, http://dx.doi.org/10.1039/C5MH00260E.

[81] K.S. Suslick, Sonochemistry, Science 247 (1990) 1439–1445, doi:10.1126/science.247.4949.1439.

[82] J.H. Bang, K.S. Suslick, Applications of ultrasound to the synthesis of nanostructured materials, Adv. Mater. 22 (2010) 1039–1059, http://dx.doi.org/10.1002/adma.200904093.

[83] J. Pinkas, V. Reichlova, R. Zboril, Z. Moravec, P. Bezdicka, J. Matejkova, Sonochemical synthesis of amorphous nanoscopic iron(III) oxide from $Fe(acac)_3$, Ultrason. Sonochem. 15 (2008) 257–264, http://dx.doi.org/10.1016/j.ultsonch.2007.03.009.

[84] O. Pascu, E. Carenza, M. Gich, S. Estradé, F. Peiro, G. Herranz, A. Roig, Surface reactivity of iron oxide nanoparticles by microwave-assisted synthesis; comparison with the thermal decomposition route, J. Phys. Chem. C 116 (2012) 15108–15116, http://dx.doi.org/10.1021/jp303204d.

[85] L. Cabrera, S. Gutierrez, N. Menendez, M.P. Morales, P. Herrasti, Magnetite nanoparticles: electrochemical synthesis and characterization, Electrochim. Acta 53 (2008) 3436–3441, http://dx.doi.org/10.1016/j.electacta.2007.12.006.

[86] W. Wu, Q. He, C. Jiang, Magnetic iron oxide nanoparticles: synthesis and surface functionalization strategies, Nanosc. Res. Lett. 3 (2008) 397–415, http://dx.doi.org/10.1007/s11671-008-9174-9.

[87] A. Shavel, L.M. Liz-Marzan, Shape control of iron oxide nanoparticles, Phys. Chem. Chem. Phys. 11 (2009) 3762–3766, http://dx.doi.org/10.1039/B822733K.

[88] R. Strobel, S.E. Pratsinis, Direct synthesis of maghemite, magnetite and wustite nanoparticles by flame spray pyrolysis, Adv. Powder Technol. 20 (2009) 190–194, http://dx.doi.org/10.1016/j.apt.2008.08.002.

[89] A. Malumbres, G. Martinez, R. Mallada, J.L. Hueso, O. Bomati-Miguel, J. Santamaria, Continuous production of iron-based nanocrystals by laser pyrolysis Effect of operating variables on size, composition and magnetic response, Nanotechnology 24 (2013) 325603, http://dx.doi.org/10.1088/0957-4484/24/32/325603.

[90] Z. Jing, S. Wu, Synthesis and characterization of monodisperse hematite nanoparticles modified by surfactants via hydrothermal approach, Mater. Lett. 58 (2004) 3637–3640, http://dx.doi.org/10.1016/j.matlet.2004.07.010.

[91] L. Yan, S. Zhang, P. Chen, H. Liu, H. Yin, H. Li, Magnetotactic bacteria, magnetosomes and their application, Microb. Res. 167 (2012) 507–519, http://dx.doi.org/10.1016/j.micres.2012.04.002.

[92] J.J. Jacob, K. Suthindhiran, Magnetotactic bacteria and magnetosomes – scope and challenges, Mater. Sci. Eng. C 68 (2016) 919–928, http://dx.doi.org/10.1016/j.msec.2016.07.049.

[93] G. Vargas, J. Cypriano, T. Correa, P. Leao, D. A: Bazylinski, F. Abreu, Applications of magnetotactic bacteria, magnetosomes and magnetosome crystals in biotechnology and nanotechnology: mini-review, Molecules 23 (2018) 2438, doi:10.3390/molecules23102438.

[94] A. Lohße, S. Borg, O. Raschdorf, I. Kolinko, E. Tompa, M. Posfai, D. Faivre, J. Baumgartner, D. Schuler, Genetic dissection of the *mam*AB and *mms*6 operons reveals a gene set essential for magnetosome biogenesis in *Magnetospirillum gryphiswaldense*, J. Bacteriol. 196 (2014) 2658–2669, doi:10.1128/JB. 01716-14.

[95] A. Curcio, A. Van de Walle, A. Serrano, S. Preveral, C. Pechoux, D. Pignol, N. Menguy, C.T. Lefevre, A. Espinosa, C. Wilhelm, Transformation cycle of magnetosomes in human stem cells: from degradation to biosynthesis of magnetic nanoparticles anew, ACS Nano (2019), http://dx.doi.org/10.1021/acsnano.9b08061 (in press).

[96] A.C.V. Araujo, F. Abreu, K.T. Silva, D.A. Bazylinski, U. Lins, Magnetotactic bacteria as potential sources of bioproducts, Marine Drugs 13 (2015) 389–430, doi:10.3390/md13010389.

[97] Z. Xu, Z. Wei, P. He, X. Duan, Z. Yang, T. Zhou, D. Jia, Seed-mediated growth of ultra-thin triangular magnetite nanoplates, Chem. Commun. 53 (2017) 11052–11055, http://dx.doi.org/10.1039/C7CC05723G.

[98] A. Espinosa, A. Munoz-Noval, M. Garcia-Hernandez, A. Serrano, J. Jimenez de la Morena, A. Figuerola, A. Quarta, T. Pellegrino, C. Wilhelm, M.A. Garcia, Magnetic properties of iron oxide nanoparticles prepared by seeded-growth route, J. Nanopart. Res. 15 (2013) 1514, http://dx.doi.org/10.1007/s11051-013-1514-8.